

Gravity-capillary waves modulated by linear shear flow in arbitrary water depth

Shaofeng Li(李少峰), Jinbao Song(宋金宝), and Anzhou Cao(曹安州)
Citation: Chin. Phys. B, 2020, 29 (**12**): 124702. DOI: 10.1088/1674-1056/abb3e4
Journal homepage: http://cpb.iphy.ac.cn; http://iopscience.iop.org/cpb

What follows is a list of articles you may be interested in

A nonlinear Schrödinger equation for gravity waves slowly modulated by linear shear flow

Shaofeng Li(李少峰), Juan Chen(陈娟), Anzhou Cao(曹安州), Jinbao Song(宋金宝)
Chin. Phys. B, 2019, 28 (**12**): 124701. DOI: 10.1088/1674-1056/ab53cf

Characteristics and generation of elastic turbulence in a three-dimensional parallel plate channel using direct numerical simulation

Hong-Na Zhang(张红娜), Feng-Chen Li(李凤臣), Xiao-Bin Li(李小斌), Dong-Yang Li(李东阳), Wei-Hua Cai(蔡伟华), Bo Yu(宇波)
Chin. Phys. B, 2016, 25 (**9**): 094701. DOI: 10.1088/1674-1056/25/9/094701

An improved element-free Galerkin method for solving generalized fifth-order Korteweg-de Vries equation

Feng Zhao, Wang Xiao-Dong, Ouyang Jie
Chin. Phys. B, 2013, 22 (**7**): 074704. DOI: 10.1088/1674-1056/22/7/074704

Gravity-capillary waves modulated by linear shear flow in arbitrary water depth*

Shaofeng Li(李少峰), Jinbao Song(宋金宝)†, and Anzhou Cao(曹安州)‡

Ocean College, Zhejiang University, Zhoushan 316000, *China*

(Received 27 May 2020; revised manuscript received 13 July 2020; accepted manuscript online 1 September 2020)

Considering that the fluid is inviscid and incompressible and the flow is irrotational in a fixed frame of reference and using the multiple scale analysis method, we derive a nonlinear Schrödinger equation (NLSE) describing the evolution dynamics of gravity-capillary wavetrains in arbitrary constant depth. The gravity-capillary waves (GCWs) are influenced by a linear shear flow (LSF) which consists of a uniform flow and a shear flow with constant vorticity. The modulational instability (MI) of GCWs with the LSF is analyzed using the NLSE. The MI is effectively modified by the LSF. In infinite depth, there are four asymptotes which are the boundaries between MI and modulational stability (MS) in the instability diagram. In addition, the dimensionless free surface elevation as a function of time for different dimensionless water depth, surface tension, uniform flow and vorticity is exhibited. It is found that the decay of free surface elevation and the steepness of free surface amplitude change over time, which are greatly affected by the water depth, surface tension, uniform flow and vorticity.

Keywords: gravity-capillary waves, nonlinear Schrödinger equation, linear shear flow, modulational instability

PACS: 47.35.Fg, 47.35.Pq, 92.10.Hm **DOI:** 10.1088/1674-1056/abb3e4

1. Introduction

Surface waves are a common oceanic phenomenon. One of them is gravity-capillary waves (GCWs) produced by the combined action of gravity and surface tension. The GCWs are usually superimposed on long gravity waves and their wavelengths range from a few millimeters to a few centimeters.[1] GCWs are a crucial factor affecting the momentum, heat and matter transfer at the air-sea interface. Therefore, the study of GCWs is of great significance for ocean remote sensing and air-sea interaction.[2] In 1968, Zakharov[3] first derived a nonlinear Schrödinger equation (NLSE) in the context of three-dimensional water wavetrains. He studied the instability of nonlinear gravity waves in deep water. In 1969, Benney and Roskes[4] first developed the modulation theory for three-dimensional gravity wavetrains. Hasimoto and Ono[5] investigated the nonlinear modulation of two-dimensional gravity wavetrains with arbitrary constant depth using singular perturbation methods. It was shown that complicated water wave equations can be reduced to an NLSE for the lowest order of perturbation, and the modulational instability (MI) is fully decided by the sign of two coefficients in the NLSE. Davey and Stewartson,[6] using the multiple scales analysis method, derived two coupled nonlinear partial differential equations which can be converted into the NLSE when the three-dimensionality is reduced to two-dimensionality. They developed the theory for three-dimensional gravity wavetrains parallel to that of Hasimoto and Ono.[5] As Benney and Roskes[4] and Davey and Stewartson[6] derived the same equations, now these equations are called the Benney–Roskes–Davey–Stewartson system. Djordjevic and Redekopp[7] combined the work of Hasimoto and Ono[5] with Davey and Stewartson[6] to consider the influence of surface tension. They studied the two-dimensional GCW trains with arbitrary constant depth. Their analysis revealed a resonant interaction between long gravity waves and short GCWs. Li *et al.*[8] and Thomas *et al.*[9] also developed the study of Hasimoto and Ono[5] and Davey and Stewartson[6] to consider the effect of nonzero constant vorticity. The theory and laboratory experiments of Li *et al.*[8] showed that small vorticity enhances MI whereas large vorticity suppresses it. Thomas *et al.*[9] demonstrated that the vorticity significantly modifies MI of gravity waves by analyzing the influences of the vorticity on the stability properties of nonlinear wave packets. Hsu *et al.*[10] combined the work of Djordjevic and Redekopp[7] with Thomas *et al.*,[9] and they found that the MI of GCWs can be modified effectively by the vorticity. Li *et al.*[11] took into account the linear shear flow (LSF) and expanded the outcomes of Thomas *et al.*[9] They pointed out that free surface elevation and the MI of gravity waves are modified greatly by the LSF which is composed of the uniform flow and the constant vorticity. The influence of vorticity on the MI and free surface elevation can be balanced

*Project supported by the National Natural Science Foundation of China (Grant No. 41830533) and the National Key Research and Development Program of China (Grant Nos. 2016YFC1401404 and 2017YFA0604102).

†Corresponding author. E-mail: songjb@zju.edu.cn

‡Corresponding author. E-mail: caoanzhou@zju.edu.cn

© 2020 Chinese Physical Society and IOP Publishing Ltd

out by that of uniform flow. Note that MI of gravity wave and GCW trains in two- and three-dimensional irrotational flows have been widely investigated before. However, in the presence of an LSF, researchers usually only considered the two-dimensional problem and the only exception is Abid *et al.*[12] who focused on the transverse instability of solitary GCWs propagating on an LSF. In this paper, we extend the results of Li *et al.*[11] to include the surface tension, and show the MI of GCWs modified by an LSF.

The MI of GCWs has been developed numerically by some scholars.[13–18] Longuet-Higgins[16] proved the presence of solitary GCWs without vorticity in deep water. Kang and Vanden-Broeck[17] obtained numerical solutions for solitary GCWs with vorticity in arbitrary constant depth. Using the NLSE and direct numerical simulations of the full Euler equations, Gao *et al.*[18] considered the MI of GCWs and solitary GCWs in finite depth with an LSF. Some other model equations were developed to numerically analyze MI of both three-dimensional and two-dimensional solitary GCWs in deep water by Akers and Milewski,[19,20] Wang,[21] and Milewski.[22] Furthermore, solitary GCWs have been researched by experiments.[23–27] For example, Zhang, using laboratory experiments in a tank[26] and field experiments in the California coastal water,[27] observed solitary GCWs which were consistent with the numerical results of Vanden-Broeck and Dias[15] and Longuet-Higgins.[16] It was found that steep short GCWs are featured by flat crests and sharp troughs, and most GCWs are far less than the critical waveform based on weak wind conditions.

The present study focuses on the MI of GCWs with an LSF and shows the dimensionless free surface elevation changes over time for the dimensionless water depth, surface tension, uniform flow and vorticity using the NLSE. In section 2, based on the multiple scale analysis method, the NLSE describing the evolution dynamics of GCW trains with the LSF in arbitrary constant depth is derived. In Section 3, the MI of GCWs is analyzed, and stability diagrams for GCWs modified by the LSF are presented. In section 4, the influences of water depth, surface tension, uniform flow and vorticity on the free surface elevation and amplitude of GCWs are explored. In Section 5, the conclusions are given.

2. Derivation of the NLSE

Assuming that the fluid is inviscid and incompressible, and the flow is irrotational. We consider a case in which two-dimensional GCW trains propagate in a finite water depth, with the existence of LSF. A fixed frame of Cartesian coordinate (Oxy) with unit vectors ($\boldsymbol{i}$, $\boldsymbol{j}$) is adopted, as presented in Fig. 1. In the figure, the x axis is aligned with the propagation direction of the wave trains, the y axis is oriented upward. Thus the gravitational acceleration is $\boldsymbol{g} = -g\boldsymbol{j}$ with $g > 0$. Without loss of generality, it is assumed that the waves propagate along the positive x axis. Here, the uniform background flows against or along the direction of wave propagation are referred to as up-flow and down-flow, respectively.

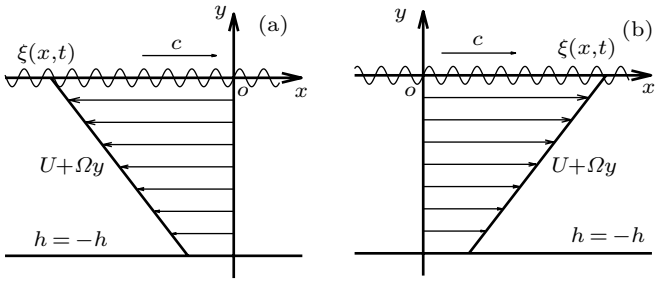


Fig. 1. Sketch of the Cartesian coordinate for two-dimensional propagating GCWs with LSF. Here c is the wave velocity and $\zeta(x,t)$ is the free surface elevation. (a) Waves propagating with negative vorticity ($\Omega < 0$) and uniform up-flow ($U < 0$). (b) Waves propagating with positive vorticity ($\Omega > 0$) and uniform down-flow ($U > 0$).

Thereafter, the governing equations of GCWs with the LSF[10,11,28] are

$$\begin{aligned}
&\Delta\phi = 0, \quad -h < y < \zeta(x,t)\\
&\phi_y = 0, \quad y = -h,\\
&\zeta_t + (\phi_x + U + \Omega\zeta)\zeta_x - \phi_y = 0, \quad y = \zeta,\\
&\phi_{tx} + \phi_{ty}\zeta_x + \phi_y(\phi_{xy} + \phi_{yy}\zeta_x) + (\phi_x + U + \Omega\zeta)(\phi_{xx} + \phi_{xy}\zeta_x),\\
&+\Omega\phi_y + g\zeta_x - \frac{\upsilon}{\rho}\left[\frac{\zeta_{xxx}}{(1+\zeta_x^2)^{3/2}} - \frac{3\zeta_x\zeta_{xx}^2}{(1+\zeta_x^2)^{5/2}}\right] = 0,\\
&y = \zeta,
\end{aligned} \tag{1}$$

where Δ is the two-dimensional Laplace operator, ϕ is the velocity potential, a constant h is the water depth, $\zeta(x,t)$ is the free surface elevation and t is the time. The subscript stands for derivatives of the corresponding variable. A constant U is the uniform flow, a constant vorticity Ω is the magnitude of the linear shear. A constant υ is the surface tension coefficient and ρ is the density of fluid.

The multiple scale analysis method[6] is adopted to derive the governing equations

$$\eta = \varepsilon(x - c_g t), \quad \tau = \varepsilon^2 t, \tag{2}$$

where η and τ are the slower variables in space and time; the small parameter $\varepsilon = kA$ characterizes the steepness of the wave train; c_g, k and A are the wave group velocity, the wave number and amplitude, respectively. Hence, the new governing equations are obtained by making a Taylor approximation for surface tension and using Eq. (2) as follows:

$$\begin{aligned}
&\varepsilon^2\phi_{\eta\eta} + \phi_{yy} = 0, \quad -h < y < \zeta(\eta,\tau),\\
&\phi_y = 0, \quad y = -h,\\
&\varepsilon^2\zeta_\tau - \varepsilon c_g\zeta_\eta + \varepsilon\zeta_\eta(\varepsilon\phi_\eta + U + \Omega\zeta) - \phi_y = 0, \quad y = \zeta,\\
&\varepsilon^3\phi_{\eta\tau} - \varepsilon^2 c_g\phi_{\eta\eta} + \varepsilon^3\phi_{y\tau}\zeta_\eta - \varepsilon^2 c_g\phi_{\eta y}\zeta_\eta\\
&+(\varepsilon^3\phi_\eta + \varepsilon^2 U + \varepsilon^2\Omega\zeta)(\phi_{\eta\eta} + \phi_{\eta y}\zeta_\eta)
\end{aligned}$$

$$+\varepsilon\phi_y(\phi_{\eta y}+\phi_{yy}\zeta_\eta)+\Omega\phi_y+\varepsilon g\zeta_\eta$$
$$-\frac{\upsilon}{\rho}\left(\varepsilon^3\zeta_{\eta\eta\eta}-\frac{3}{2}\varepsilon^5\zeta_\eta^2\zeta_{\eta\eta\eta}-3\varepsilon^5\zeta_{\eta\eta}^2\zeta_\eta\right)=0,$$
$$y=\zeta. \tag{3}$$

Note Eq. (3) matches the result of Hsu *et al.*[10] when $U=0$ and of Li *et al.*[11] when $\upsilon=0$. The velocity potential ϕ is expanded in a Taylor series of ζ about $y=0$ and substituted into the upper boundary conditions of Eq. (3). An asymptotic solution of Eq. (3) is sought with the plane wave as follows:

$$\phi=\sum_{n=-\infty}^{+\infty}\phi_n\exp\left[\mathrm{i}n\left(kx-\omega t\right)\right],$$
$$\zeta=\sum_{n=-\infty}^{+\infty}\zeta_n\exp\left[\mathrm{i}n\left(kx-\omega t\right)\right], \tag{4}$$

where n is the order of harmonics and ω is the angular frequency. We assume $\phi_{-n}=\phi_n^*$ and $\zeta_{-n}=\zeta_n^*$, where the asterisk denotes the complex conjugate. Thereafter, ϕ_n and ζ_n are expanded in a power series of ε:

$$\phi_n=\sum_{m=n}^{+\infty}\varepsilon^m\phi_{nm}(\eta,y,\tau),\quad \zeta_n=\sum_{m=n}^{+\infty}\varepsilon^m\zeta_{nm}(\eta,\tau). \tag{5}$$

Assume $\phi_{00}=\zeta_{00}=0$ and m is the order. Substituting Eqs. (4) and (5) into Eq. (3), a set of ordinary linear differential equations for ϕ_{nm} and ζ_{nm} are obtained by separating the different orders and harmonics. The detailed derivations are succinctly given in Appendix. Here, we just exhibit the linear dispersion relation, the group velocity and the final equation and coefficients for the amplitude of ϕ.

The linear dispersion relation for $m=1$ and $n=1$ is shown as follows:

$$\omega^2\left(1+X-\bar{u}\right)\left(1-\bar{u}\right)=gk\sigma\left(1+N\right), \tag{6}$$

where

$$c=\frac{\omega}{k},\quad \bar{u}=\frac{U}{c},\quad \mu=kh,\quad \sigma=\tanh\mu,$$
$$\bar{\Omega}=\frac{\Omega}{\omega},\quad X=\sigma\bar{\Omega},\quad N=\frac{\upsilon k^2}{\rho g}. \tag{7}$$

Here, c is the wave velocity, $\bar{u}$ is the dimensionless uniform flow, μ is the dimensionless water depth, $\bar{\Omega}$ is the dimensionless vorticity, and N is the dimensionless surface tension. Generally, GCWs are short waves, which can be considered as the deep wave ($\mu\geq\pi$). Therefore, Eq. (6) becomes

$$\omega^2\left(1+\bar{\Omega}-\bar{u}\right)\left(1-\bar{u}\right)=gk\left(1+N\right). \tag{8}$$

If we select $\rho=1020$ kg/m^3, $g=9.8$ m/s^2 and $\upsilon=0.074$ N/m^2, we can find that the surface tension is as important as the gravity for $k=367.5$ m^{-1}; an order of magnitude smaller than the gravity for $k=116.2$ m^{-1}; and an order of magnitude larger than the gravity for $k=1162.2$ m^{-1}. These may be used as the basis for the classification of gravity waves, GCWs and capillary waves. Hence, the effect of surface tension on waves is not negligible for $k\geq116.2$ m^{-1}. The group velocity is

$$c_{\mathrm{g}}=\frac{\partial\omega}{\partial k}=\frac{c}{\sigma}\frac{\mu\left(1-\sigma^2\right)\left(1-\bar{u}\right)^2+\sigma\left(1+X-\bar{u}\right)\left(1-\bar{u}\right)\left(1+3N\right)/\left(1+N\right)}{2+X-2\bar{u}}+c\bar{u}. \tag{9}$$

For $m=3$ and $n=1$, the NLSE of GCWs with the LSF for the amplitude A of velocity potential is obtained as follows:

$$\mathrm{i}\frac{\partial A}{\partial\tau}+\alpha\frac{\partial^2A}{\partial\eta^2}=\beta\left|A\right|^2A, \tag{10}$$
$$\alpha=\frac{\omega\left(\alpha_1+\alpha_2\right)}{k^2\sigma\left(2+X-2\bar{u}\right)}, \tag{11}$$
$$\alpha_1=\mu\left(1-\sigma^2\right)\left[\left(1-\mu\sigma\right)\left(1-\bar{u}\right)^2+\left(1-\bar{c}_{\mathrm{g}}\right)X\right]-\sigma\left(\bar{c}_{\mathrm{g}}-\bar{u}\right)^2, \tag{12}$$
$$\alpha_2=\frac{N}{1+N}\left[3\sigma+2\mu\left(1-\sigma^2\right)\right]\left(1-\bar{u}\right)\left(1+X-\bar{u}\right), \tag{13}$$
$$\beta=\frac{k^3\omega\left(\beta_1+\beta_2+2\beta_3\beta_4+\beta_5\beta_6\right)}{2g\sigma\left(1+N\right)\left(2+X-2\bar{u}\right)}, \tag{14}$$
$$\beta_1=2\sigma^2\left(1-\bar{u}\right)\left(1+X-\bar{u}\right)\left(4+3X-4\bar{u}\right), \tag{15}$$
$$\beta_2=-\frac{3N}{1+N}\sigma^2\left(1+X-\bar{u}\right)^2-2\left(1+N\right)\left(1-\sigma^2\right)\times\left[\left(1+X-\bar{u}\right)^2-\sigma^2\left(1-\bar{u}\right)^2\right], \tag{16}$$
$$\beta_3=\left(1+N\right)\left(\sigma\bar{c}_{\mathrm{g}}-\sigma\bar{u}+\mu X\right)\times\left[\left(1+X-\bar{u}\right)^2-\sigma^2\left(1-\bar{u}\right)^2\right]+\sigma\left(1-\bar{u}\right)\left(1+X-\bar{u}\right)\left(2+X-2\bar{u}\right), \tag{17}$$
$$\beta_4=\frac{\left(1+X-\bar{u}\right)\left(2+X-2\bar{u}\right)+\left(1+N\right)\left(1-\sigma^2\right)\left(\bar{c}_{\mathrm{g}}-\bar{u}\right)\left(1-\bar{u}\right)}{\left(1-\bar{u}\right)\left[\left(\bar{c}_{\mathrm{g}}-\bar{u}\right)\left(\sigma\bar{c}_{\mathrm{g}}-\sigma\bar{u}+\mu X\right)\left(1+N\right)-\mu\left(1+X-\bar{u}\right)\left(1-\bar{u}\right)\right]}, \tag{18}$$
$$\beta_5=\left(\sigma^4-10\sigma^2+9\right)\left(1-\bar{u}\right)^2+\left(-4\sigma^4-4\sigma^2+18\right)\left(1-\bar{u}\right)X+\left(3\sigma^2+15\right)X^2+\left(2\sigma^2+6\right)\left(1-\bar{u}\right)^{-1}X^3+\left(1-\bar{u}\right)^{-2}X^4$$
$$+N[\left(\sigma^4-10\sigma^2+21\right)\left(1-\bar{u}\right)^2+\left(-4\sigma^4+2\sigma^2+42\right)\left(1-\bar{u}\right)X+\left(12\sigma^2+30\right)X^2$$
$$+\left(5\sigma^2+9\right)\left(1-\bar{u}\right)^{-1}X^3+\left(1-\bar{u}\right)^{-2}X^4], \tag{19}$$

$$\beta_6 = \frac{1+X-\bar{u}}{\sigma^2(1-\bar{u})(1+N)-3N(1+X-\bar{u})}. \tag{20}$$

Here $\bar{c}_g = c_g/c$ is the dimensionless group velocity, α and β are the dispersion and nonlinear coefficients, respectively, which depend on ($\bar{u}$, X, μ, N). If $\bar{u}=0$, Eqs. (10)–(20) can be reduced to those of Hsu *et al.*[10] If $N=0$, they can be obtained similarly to Li *et al.*[11] Note that Eq. (18) shows the coupling between LSF and the induced slowly varying mean flow (ϕ_{01}). It is found that there are two singularities in the nonlinear coefficient. The one is

$$N = \frac{\sigma^2(1-\bar{u})}{3(1+X-\bar{u})-\sigma^2(1-\bar{u})}. \tag{21}$$

It reflects the phenomenon of Wilton ripple that corresponds to a bifurcation of GCWs. The other is

$$\begin{aligned}&(\bar{c}_g-\bar{u})(\sigma\bar{c}_g-\sigma\bar{u}+\mu X)(1+N)\\&-\mu(1+X-\bar{u})(1-\bar{u})=0,\end{aligned} \tag{22}$$

i.e., the dimensional form is

$$(c_g-U)(c_g-U+\Omega h)=gh. \tag{23}$$

Equations (22) and (23) reflect the resonance between long gravity waves and short GCWs. The wave velocity of long gravity waves matches the group velocity of GCWs.

In order to analyze the amplitude B of the free surface elevation. We set[10]

$$\begin{aligned}\zeta &= \mathrm{Re}\left(\varepsilon B\mathrm{e}^{\mathrm{i}(kx-\omega t)}\right)+O(\varepsilon^2)\\&=\frac{1}{2}(\varepsilon B\mathrm{e}^{\mathrm{i}(kx-\omega t)}+\mathrm{c.c.})+O(\varepsilon^2),\end{aligned} \tag{24}$$

where Re denotes real part and c.c. denotes complex conjugation. From Eqs. (A7), (4), and (5), we know

$$\begin{aligned}\zeta &= \left(\varepsilon\zeta_{11}\mathrm{e}^{\mathrm{i}(kx-\omega t)}+\mathrm{c.c.}\right)+O(\varepsilon^2)\\&=\left(\varepsilon\frac{\mathrm{i}\sigma}{c(1-\bar{u})}A\mathrm{e}^{\mathrm{i}(kx-\omega t)}+\mathrm{c.c.}\right)+O(\varepsilon^2).\end{aligned} \tag{25}$$

Equations (24) and (25) are equal, hence

$$\frac{\mathrm{i}\sigma}{c(1-\bar{u})}A=\frac{1}{2}B=\zeta_{11}. \tag{26}$$

Substituting Eq. (26) into Eq. (10), we obtain

$$\mathrm{i}\frac{\partial B}{\partial\tau}+\alpha\frac{\partial^2 B}{\partial\eta^2}=\gamma|B|^2B, \tag{27}$$

where

$$\gamma=\frac{c^2(1-\bar{u})^2}{4\sigma^2}\beta. \tag{28}$$

When the dimensionless water depth is infinite, the coefficients of the NLSEs (9) and (11)–(20) with the LSF become

$$\bar{c}_g = \frac{(1+\bar{\Omega}-\bar{u})(1-\bar{u})(1+3N)}{(2+\bar{\Omega}-2\bar{u})(1+N)}+\bar{u}, \tag{29}$$

$$\begin{aligned}\alpha &= \frac{\omega(1+\bar{\Omega}-\bar{u})(1-\bar{u})}{k^2(2+\bar{\Omega}-2\bar{u})(1+N)}\\&\times\left[3N-\frac{(1+\bar{\Omega}-\bar{u})(1-\bar{u})(1+3N)^2}{(2+\bar{\Omega}-2\bar{u})^2(1+N)}\right],\end{aligned} \tag{30}$$

$$\begin{aligned}\gamma &= \frac{\omega k^2(1-\bar{u})}{8(1+\bar{\Omega}-\bar{u})(2+\bar{\Omega}-2\bar{u})}\\&\times\left\{2(1+\bar{\Omega}-\bar{u})(4+3\bar{\Omega}-4\bar{u})-\frac{3N}{1+N}(1+\bar{\Omega}-\bar{u})^2\right.\\&+\frac{2\bar{\Omega}^2(1+N)(2+\bar{\Omega}-2\bar{u})^3}{(1-\bar{u})^2[3N\bar{\Omega}-2(1-\bar{u})]}\\&\left.+\frac{1+\bar{\Omega}-\bar{u}}{(1-\bar{u})(1-2N)-3N\bar{\Omega}}\beta_5\right\},\end{aligned} \tag{31}$$

$$\begin{aligned}\beta_5 &= 10(1-\bar{u})\bar{\Omega}+18\bar{\Omega}^2+8(1-\bar{u})^{-1}\bar{\Omega}^3+(1-\bar{u})^{-2}\bar{\Omega}^4\\&+N[12(1-\bar{u})^2+40(1-\bar{u})\bar{\Omega}+42\bar{\Omega}^2\\&+14(1-\bar{u})^{-1}\bar{\Omega}^3+(1-\bar{u})^{-2}\bar{\Omega}^4].\end{aligned} \tag{32}$$

The resonance curves' Eqs. (21)–(23) become

$$N=\frac{(1-\bar{u})}{3\bar{\Omega}+2(1-\bar{u})}, \tag{33}$$

$$N=\frac{2(1-\bar{u})}{3\bar{\Omega}}, \tag{34}$$

$$\Omega(c_g-U)=g. \tag{35}$$

In this work, we only consider the subcritical flow with $|\bar{u}|<1$. According to Eq. (6), we can find $X>\bar{u}-1$. In the infinite depth, it is $\Omega>\bar{u}-1$.

3. Modulational instability analysis

As we learn that the sign of the product of $\alpha\gamma$ of the NLSE decides whether GCWs are stable on infinitesimal perturbations.[29,30] If the sign of $\alpha\gamma$ is positive, the GCWs corresponding to the defocusing NLSE are modulationally stable, otherwise the GCWs corresponding to the focusing NLSE are modulationally unstable.[31,32]

Figure 2(a) shows the unstable and stable regions of gravity waves in the (X,μ) space for different $\bar{u}$. Figure 2(b) displays the unstable and stable regions of the GCWs without LSF in the (N,μ) space. As a verification, Figure 2(a) is compared with that of Li *et al.*[11] Figure 2(b) is compared with that of Ablowitz *et al.*[33] and Hsu *et al.*[10] In Fig. 2(a), without considering the surface tension, the neutral curve denotes $\alpha\gamma=0$, which divides the (X,μ) space into stable region if the corresponding parameters (X,μ) locates below the neutral curve, and unstable region if (X,μ) locates above the neutral

curve for each $\bar{u}$. These neutral curves have a node $\mu = 1.363$, which determines whether the gravity wave is stable.[34] It is also seen that the neutral curve moves to the right with the increase of $\bar{u}$, i.e., the unstable region becomes smaller. In Fig. 2(b), the five curves divide the (N,μ) plane into six regions, where the stability and instability are exchanged in turn from left to right. The dotted line $\gamma = 0$ indicates the disappearance of nonlinear coefficient, the dashed line $\alpha = 0$ indicates the disappearance of dispersion coefficient, the dot-dashed line shows the singularity of Eq. (21), the solid line shows the singularity of Eqs. (22) and (23).

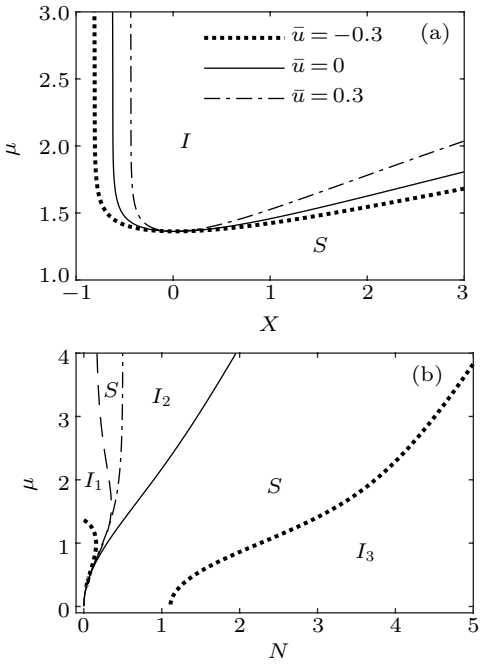


Fig. 2. (a) The (X,μ)-stability diagram for gravity waves with different uniform flows. (b) The (N,μ)-stability diagram for GCWs without the LSF. S denotes stability, I and I_j $(j = 1, 2, 3)$ denote instability.

As shown in Fig. 3, the uniform flow and the vorticity can effectively affect the (N,μ)-stability diagram for GCWs. In Figs. 3(a) and 3(b), the negative vorticity deflects five neutral curves to the right corresponding to the six regions moving to the right whereas the positive vorticity deflects five neutral curves to the left corresponding to the six regions moving to the left, whatever the uniform flow is up-flow or down-flow (therefore we only show the result corresponding to $\bar{u} = 0$). For negative vorticity, as shown in Figs. 3(c) and 3(d), the uniform up-flow deflects neutral curves to the left while the uniform down-flow deflects neutral curves to the right. However, for positive vorticity, they have a reverse change, as shown in Figs. 3(e) and 3(f). In the absence of vorticity, the stability diagram is independent of the uniform flow, as shown in Fig. 2(b). This means that the uniform flow has an effect on the stability diagram only when it interacts with the vorticity. In Figs. 3(g) and 3(h), the two sets of curves coincide, which means that the influence of vorticity on the MI can be balanced out by that of uniform flow. When the vorticity is negative, it can be balanced out by uniform up-flow, as shown in Fig. 3(g). When the vorticity is positive, it can also be balanced out by uniform up-flow, as shown in Fig. 3(h).

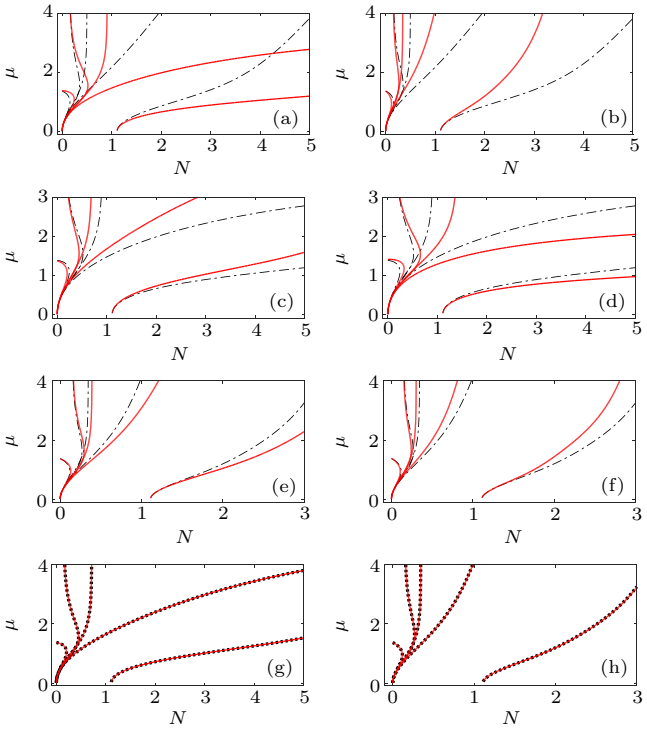


Fig. 3. The (N,μ)-stability diagram for GCWs: (a) $\bar{u} = 0$ for $\bar{\Omega} = 0$ (dot-dashed) and $\bar{\Omega} = -0.3$ (red); (b) $\bar{u} = 0$ for $\bar{\Omega} = 0$ (dot-dashed) and $\bar{\Omega} = 0.3$ (red); (c) $\bar{\Omega} = -0.3$ for $\bar{u} = 0$ (dot-dashed) and $\bar{u} = -0.6$ (red); (d) $\Omega = -0.3$ for $\bar{u} = 0$ (dot-dashed) and $\bar{u} = 0.3$ (red); (e) $\bar{\Omega} = 0.3$ for $\bar{u} = 0$ (dot-dashed) and $\bar{u} = -0.6$ (red); (f) $\bar{\Omega} = 0.3$ for $\bar{u} = 0$ (dot-dashed) and $\bar{u} = 0.3$ (red); (g) $\bar{u} = 0$ for $\bar{\Omega} = -0.2$ (dotted), and $\bar{u} = -0.5$ for $\bar{\Omega} = -0.3$ (red); (h) $\bar{u} = 0$ for $\bar{\Omega} = 0.3$ (dotted), and $\bar{u} = 0.33$ for $\bar{\Omega} = 0.2$ (red).

Generally, the surface tension is not negligible when the wavelength is short enough ($k \geq 116.2$ m^{-1}). Therefore, GCWs and capillary waves can be seen as waves of infinite depth. As exhibited in Fig. 4, the $(N,\bar{\Omega})$ plane is divided into seven regions by five critical curves, where the stability and instability are exchanged in turn. The two dotted lines indicate simple zeros of the nonlinear coefficient. The solid line indicates simple zero of the dispersion coefficient. The dot-dashed line shows a bifurcation of GCWs. The dashed line shows the resonance between long gravity waves and short GCWs. In Fig. 4(a), as the surface tension increases, the dotted line which has the asymptote $\bar{\Omega} = -0.688$ and the dot-dashed line which has the asymptote $\bar{\Omega} = -0.667$ almost overlap. Therefore, there is a very thin band of stability between them. The dashed line and dotted line almost coincide and have the asymptote $\bar{\Omega} = 0$ with the increase of the surface tension; the stable band between them disappears. The dotted line has another asymptote $\bar{\Omega} = 5.29$. This means that GCWs are stable when $\bar{\Omega} > 5.29$, except that N is very small. The solid line, the dot-dashed line and the dashed line coincide as the vortic-

ity increases. They have the asymptote $N=0$. This means that the stable and unstable bands disappear among them.

Figure 5 shows the influence of uniform flow on the $(N,\bar{\Omega})$ plane in the infinite depth. There are four asymptotes $\bar{\Omega}=-0.688(1-\bar{u})$, $\bar{\Omega}=-0.667(1-\bar{u})$, $\bar{\Omega}=0$ and $\bar{\Omega}=5.29(1-\bar{u})$ on the plane as the surface tension increases. As shown in Figs. 5(a)–5(c), the down-flow makes the neutral curves move to the downside when the vorticity is positive, whereas it makes the neutral curves move to the upside when the vorticity is negative. From Fig. 5(c), the down-flow makes asymptote move to the downside for positive vorticity, keeps asymptote still without the vorticity, makes asymptote move to the upside for negative vorticity. However, as shown in Figs. 5(d)–5(f), the up-flow makes the neutral curves move to the upside for positive vorticity and to the downside for negative vorticity; the up-flow makes asymptote move to the upside for positive vorticity, keeps asymptote still without the vorticity, makes asymptote move to the downside for negative vorticity.

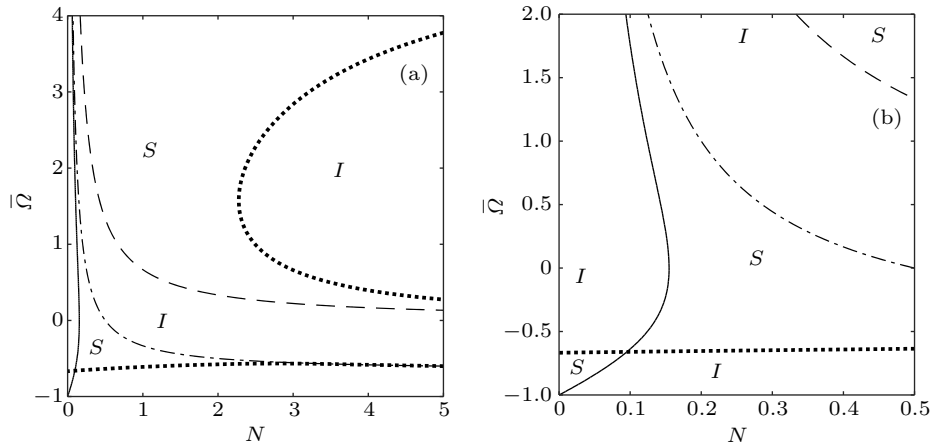


Fig. 4. The $(N,\bar{\Omega})$-stability diagram for GCWs in the infinite depth with $\bar{u}=0$. S and I denote stability and instability. (a) $(N,\bar{\Omega})\in[0,5]\times(-1,4]$. (b) Part of the (a) for $(N,\bar{\Omega})\in[0,0.5]\times(-1,2]$.

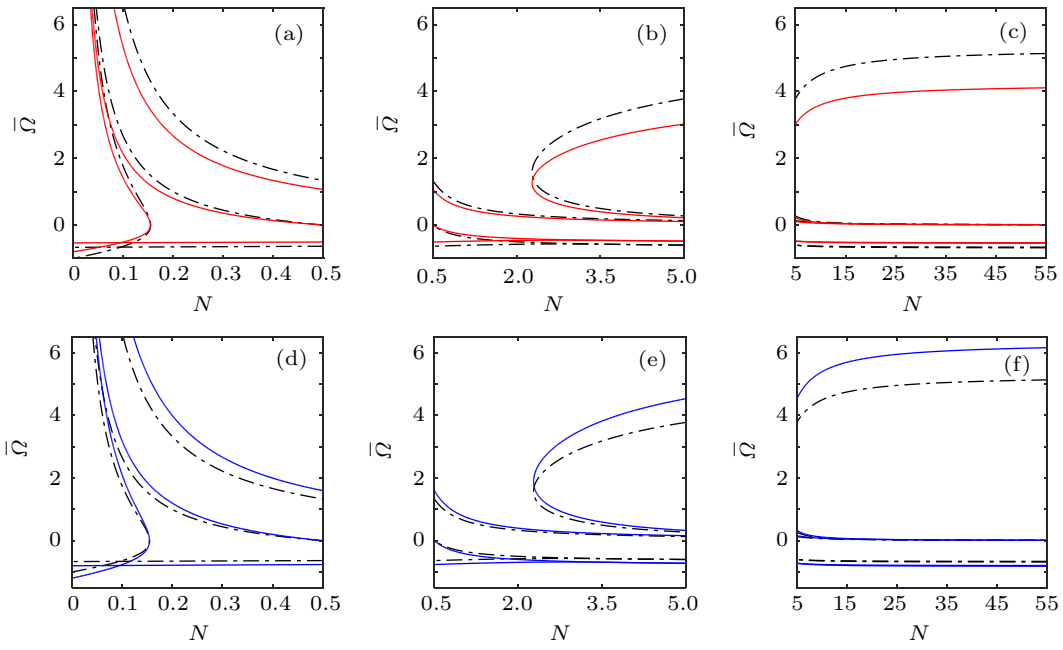


Fig. 5. The $(N,\bar{\Omega})$-stability diagram for GCWs in the infinite depth: $\bar{u}=0.2$ (red), $\bar{u}=0$ (dot-dashed), $\bar{u}=-0.2$ (blue); (a) and (d) $N\in[0,0.5]$, (b) and (e) $N\in[0.5,5]$, (c) and (f) $N\in[5,55]$.

4. Application

The NLSE model is used to study solitary GCWs in the presence of the LSF. Equation (27) has the following solution:[12,35]

$$B=B_0\,\mathrm{sech}\left(\sqrt{-\frac{\gamma}{2\alpha}}B_0\eta\right)\exp\left(-\frac{\mathrm{i}}{2}\gamma B_0^2\tau\right), \tag{36}$$

where B_0 is the initial amplitude. The free surface elevation of solitary GCWs in the first order approximation is expressed as

$$\zeta = \varepsilon B_0\,\mathrm{sech}\left[\sqrt{-\frac{\gamma}{2\alpha}}\varepsilon B_0\left(x-c_g t\right)\right] \times\cos\left[kx-\left(\omega+\frac{\gamma}{2}\varepsilon^2B_0^2\right)t\right]. \tag{37}$$

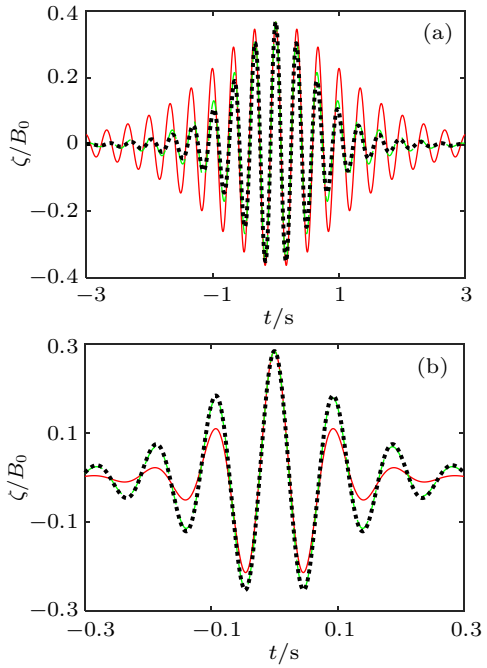


Fig. 6. The dimensionless free surface elevation as a function of time with $x = 0$ m, $\bar{u} = 0$, $\bar{\Omega} = 0$ for $\mu = 2$ (red solid), $\mu = 5$ (green dashed), $\mu = +\infty$ (black dotted). (a) $N = 0.01$, $B_0 = 1$ cm. (b) $N = 0.6$, $B_0 = 0.1$ cm.

In Fig. 2(b), the dashed line and dot-dashed line have the asymptotes $N = 2/3^{1/2} - 1$ and $N = 1/2$, respectively.[10] Figure 6 shows that the dimensionless free surface elevation as a function of time for different water depths at $N = 0.01$, which belongs to I_1 of Fig. 2(b) and that at $N = 0.6$ which belongs to I_2 of Fig. 2(b). Here, the free surface waves are assumed to come from negative time. Figure 6(a) shows that the steepness of free surface amplitude becomes larger and the free surface elevation decays faster with time as the water depth increases, but Fig. 6(b) shows that they have opposite changes as the water depth increases. In addition, as presented in Fig. 6, the coincidence between the green dashed line and the black dotted line indicates that the effect of water depth on the free surface elevation and amplitude can be neglected when $\mu \geq 5$.

Figure 7 shows the dimensionless free surface elevation as a function of time without the LSF for different surface tensions in the infinite depth. The waveform (Eq. 35) at $x = 0$ m is symmetric with respect to time, so only the free surface elevation at a positive time is shown. For both I_1 and I_2, the surface tension becomes larger with the increase of the wave number. Hence, when the initial amplitude is fixed, as shown in Fig. 7, both the height and steepness of free surface amplitude increase, which means that the nonlinear effect becomes stronger with the increase of the surface tension. Moreover, the free surface elevation decays faster with time as the surface tension increases.

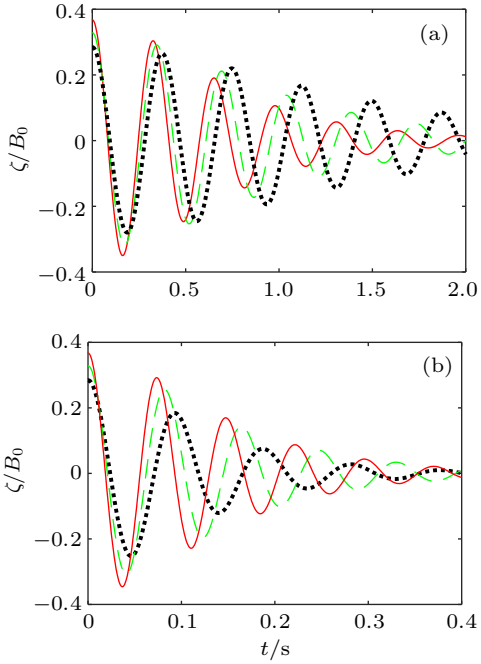


Fig. 7. The dimensionless free surface elevation as a function of time with $x = 0$ m, $\mu = +\infty$, $\bar{u} = 0$, $\bar{\Omega} = 0$. (a) $B_0 = 1$ cm for $N = 0.01$ (red solid), $N = 0.008$ (green dashed), $N = 0.006$ (black dotted). (b) $B_0 = 0.1$ cm for $N = 1$ (red solid), $N = 0.8$ (green dashed), $N = 0.6$ (black dotted).

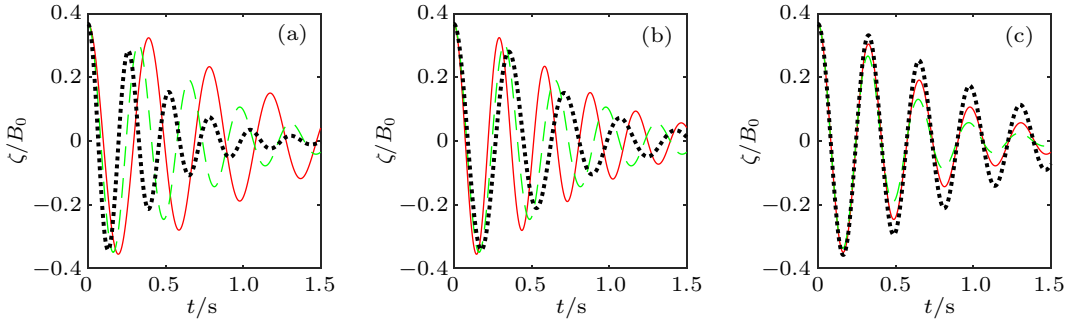


Fig. 8. The dimensionless free surface elevation as a function of time with $x = 0$ m, $B_0 = 1$ cm, $N = 0.01$, $\mu = +\infty$: (a) $\bar{\Omega} = 0$ for $\bar{u} = -0.2$ (red solid), and $\bar{u} = 0$ (green dashed) for $\bar{u} = 0.2$ (black dotted); (b) $\bar{u} = 0$ for $\bar{\Omega} = -0.2$ (red solid), $\bar{\Omega} = 0$ (green dashed), $\bar{\Omega} = 0.2$ (black dotted); (c) $\bar{u} = 0$ for $\bar{\Omega} = 0$ (red solid), $\bar{u} = 0.1$ for $\bar{\Omega} = 0.2$ (green dashed), and $\bar{u} = -0.1$ for $\bar{\Omega} = -0.2$ (black dotted).

Figure 8 shows the dimensionless free surface elevation as a function of time with the constant surface tension for different uniform flows and vorticity in the infinite depth. As exhibited in Fig. 8(a), uniform up-flow decreases the steepness of free surface amplitude, while uniform down-flow increases it. The free surface elevation decays faster with time as the uniform flow increases. As presented in Fig. 8(b), negative vorticity increases the steepness of free surface amplitude,

whereas positive vorticity decreases it. The free surface elevation decays faster with time as the vorticity decreases. Hence, the influence of uniform flow on the free surface elevation and the steepness of free surface amplitude is the opposite to that of vorticity. As shown in Fig. 8(c), the coincidence between the green dashed line and the red solid line suggests that the effect of uniform down-flow on the free surface elevation and the steepness of free surface amplitude can be offset by the positive vorticity, the coincidence between the black dotted line and the red solid line means that the effect of uniform up-flow on the free surface elevation and the steepness of free surface amplitude can be offset by the negative vorticity.

5. Conclusion

The two-dimensional NLSE describing the evolution of GCW trains in arbitrary constant depth with an LSF has been derived using the multiple scale analysis method. Based on the sign of the product of $\alpha\gamma$ which depends on $(\bar{u},X,\mu,N)$ of the NLSE, the unstable ($\alpha\gamma<0$) and stable ($\alpha\gamma>0$) regions with respect to (N,μ) for different uniform and vorticity are shown by analyzing the MI. It is found that negative vorticity deflects five neutral curves ($\alpha=0$, $\gamma=0$, two singularities) to the right whereas positive vorticity deflects them to the left in the (N,μ) diagram. For negative vorticity, uniform up-flow deflects five neutral curves to the left while uniform down-flow deflects five neutral curves to the right. However, for positive vorticity, they have a reverse change. Hence, the influence of vorticity on the MI can be balanced out by that of uniform flow. In the absence of vorticity, the stability diagram is independent of the uniform flow.

In infinite depth, the $(N,\bar{\Omega})$ instability diagrams for different uniform flow show four asymptotes $\bar{\Omega}=-0.688(1-\bar{u})$, $\bar{\Omega}=-0.667(1-\bar{u})$, $\bar{\Omega}=0$ and $\bar{\Omega}=5.29(1-\bar{u})$ as the surface tension goes to infinity. It is found that, for negative vorticity, down-flow makes the neutral curves move to the upside whereas up-flow makes them move to the downside. However, for positive vorticity, they also have a reverse change. In the absence of vorticity, they are unchanged in the $(N,\bar{u})$ instability diagram.

The NLSE model is used to study solitary GCWs in the presence of an LSF. It is shown that the steepness of free surface amplitude becomes larger and the free surface elevation decays faster with time as the water depth increases when N belongs to I_1. However, they have opposite changes when N belongs to I_2. Moreover, the effect of water depth on the free surface elevation and amplitude can be neglected when $\mu\geq 5$.

In infinite depth, both the height and steepness of free surface amplitude increase as well as the free surface elevation decays faster with time as the surface tension increases. Furthermore, uniform up-flow decreases the steepness of free surface amplitude, while uniform down-flow increases it. Negative vorticity increases the steepness of free surface amplitude, whereas positive vorticity decreases it. The free surface elevation decays faster with time as the uniform flow increases, whereas it decays more slowly as the vorticity increases. Therefore, the effect of uniform down-flow (up-flow) on the free surface elevation and the steepness of free surface amplitude can be offset by the positive (negative) vorticity.

In the paper, we focus on MI of GCWs with an LSF which is the generation mechanism of solitary GCWs. The judging criterions for the occurrence of solitary GCWs in finite depth and deep water are given, as shown in Figs. 2–5. Through these stability diagrams (Figs. 2–5), parameters of dimensionless water depth, surface tension, uniform flow and vorticity are established in the unstable regions where solitary GCWs occur. Setting different parameters of unstable regions, it is found that the free surface elevation of solitary GCWs as a function of time is greatly affected by the water depth, surface tension, uniform flow and vorticity, as shown in Figs. 6–8.

Appendix A

As mentioned in the text, m is the order of series and n is the order of harmonics. For $m=1$ and $n=0$, the solutions can be obtained as follows:

$$\phi_{01y}=0. \tag{A1}$$

For $m=1$ and $n=1$, the governing equations are

$$\phi_{11yy}-k^2\phi_{11}=0,\quad -h<y<\zeta, \tag{A2}$$

$$\phi_{11y}=0,\quad y=-h, \tag{A3}$$

$$\mathrm{i}\,(\omega-kU)\,\zeta_{11}+\phi_{11y}=0,\quad y=0, \tag{A4}$$

$$k\,(\omega-kU)\,\phi_{11}+\Omega\phi_{11y}+\mathrm{i}gk\,(1+N)\,\zeta_{11}=0,$$
$$y=0, \tag{A5}$$

where $N=\upsilon k^2/\rho g$ is the dimensionless surface tension. The solutions can be obtained as follows:

$$\phi_{11}=A\frac{\cosh\left[k\,(y+h)\right]}{\cosh\,(kh)}, \tag{A6}$$

$$\zeta_{11}=\frac{\mathrm{i}\sigma}{c\,(1-\bar{u})}A=\frac{\mathrm{i}\omega\,(1+X-\bar{u})}{g\,(1+N)}A, \tag{A7}$$

where

$$c=\frac{\omega}{k},\quad \bar{u}=\frac{U}{c},\quad \mu=kh,\quad \sigma=\tanh\mu,$$
$$\bar{\Omega}=\frac{\Omega}{\omega},\quad X=\sigma\bar{\Omega}. \tag{A8}$$

Here, c is the wave velocity, $\bar{u}$ is the dimensionless uniform flow, μ is the dimensionless water depth, $\bar{\Omega}$ is the dimensionless vorticity, and N is the dimensionless surface tension. The slowly varying amplitude $A(\eta,\tau)$ of the velocity potential is used to represent all other terms.

For $m=2$ and $n=0$, the solutions can be obtained as follows:

$$\zeta_{01}=\phi_{02y}=0. \tag{A9}$$

For $m=2$ and $n=1$, the governing equations are

$$2ik\phi_{11\eta}-k^2\phi_{12}+\phi_{12yy}=0,\quad -h<y<\zeta, \tag{A10}$$
$$\phi_{12y}=0,\quad y=-h, \tag{A11}$$
$$\mathrm{i}\left(\omega-kU\right)\zeta_{12}+\left(c_{\mathrm{g}}-U\right)\zeta_{11\eta}+\phi_{12y}=0,\quad y=0, \tag{A12}$$
$$\mathrm{i}\left(2kU-kc_{\mathrm{g}}-w\right)\phi_{11\eta}+k\left(w-kU\right)\phi_{12}+\Omega\phi_{12y},$$
$$+g\left(1+3N\right)\zeta_{11\eta}+igk\left(1+N\right)\zeta_{12}=0,\quad y=0. \tag{A13}$$

The solutions can be obtained as follows:

$$\phi_{12}=D\frac{\cosh\left[k\left(y+h\right)\right]}{\cosh\left(kh\right)}-\mathrm{i}A_{\eta}\frac{\left(y+h\right)\sinh\left[k\left(y+h\right)\right]-h\sigma\cosh\left[k\left(y+h\right)\right]}{\cosh\left(kh\right)}, \tag{A14}$$

$$\zeta_{12}=\frac{1}{g\left(1+N\right)}\left[c_{\mathrm{g}}-c\bar{u}+h\left(1-\sigma^2\right)\Omega-c\left(1+X-\bar{u}\right)\frac{2N}{1+N}\right]A_{\eta}+\frac{\mathrm{i}\omega\left(1+X-\bar{u}\right)}{g\left(1+N\right)}D. \tag{A15}$$

Here, D is a slowly varying function to be determined.

For $m=2$ and $n=2$, the governing equations are

$$\phi_{22yy}-4k^2\phi_{22}=0,\quad -h<y<\zeta, \tag{A16}$$
$$\phi_{22y}=0,\quad y=-h, \tag{A17}$$
$$-2\mathrm{i}\left(\omega-kU\right)\zeta_{22}-k^2\phi_{11}\zeta_{11}-\phi_{11yy}\zeta_{11}-\phi_{22y}+\mathrm{i}k\Omega\zeta_{11}^2=0,\quad y=0, \tag{A18}$$
$$4k\left(\omega-kU\right)\phi_{22}+2k\left(\omega-kU\right)\phi_{11y}\zeta_{11}-\mathrm{i}k^3\phi_{11}^2+\mathrm{i}k\phi_{11y}^2-k^2\Omega\phi_{11}\zeta_{11}+\Omega\phi_{11yy}\zeta_{11}+\Omega\phi_{22y}$$
$$+2\mathrm{i}gk\left(1+4N\right)\zeta_{22}=0,\quad y=0. \tag{A19}$$

The solutions can be obtained as follows:

$$\phi_{22}=\frac{\mathrm{i}k^2\left(1+\sigma^2\right)}{4\omega\left(1-\bar{u}\right)^2}QA^2\frac{\cosh\left[2k\left(y+h\right)\right]}{\cosh\left(2kh\right)}, \tag{A20}$$

$$Q=\frac{\left[3\left(1-\sigma^2\right)\left(1-\bar{u}\right)^2+3X\left(1-\bar{u}\right)+X^2\right]+N\left[3\left(3-\sigma^2\right)\left(1-\bar{u}\right)^2+12X\left(1-\bar{u}\right)+4X^2\right]}{\sigma^2\left(1-\bar{u}\right)\left(1+N\right)-3N\left(1+X-\bar{u}\right)}, \tag{A21}$$

$$\zeta_{22}=-\frac{k^3\sigma\left(1+N\right)}{2\omega^2\left(1-\bar{u}\right)^3}\frac{\left(3-\sigma^2\right)\left(1-\bar{u}\right)^2+\left(3+\sigma^2\right)\left(1-\bar{u}\right)X+X^2}{\sigma^2\left(1-\bar{u}\right)\left(1+N\right)-3N\left(1+X-\bar{u}\right)}A^2. \tag{A22}$$

For $m=3$ and $n=0$, the governing equations are

$$\phi_{01\eta\eta}+\phi_{03yy}=0,\quad -h<y<\zeta, \tag{A23}$$
$$\phi_{03y}=0,\quad y=-h, \tag{A24}$$
$$-\left(c_{\mathrm{g}}-U\right)\zeta_{02\eta}+\mathrm{i}k\phi_{11}\zeta_{-11\eta}+\mathrm{i}k\zeta_{11}\phi_{-11\eta}+k^2\phi_{-11}\zeta_{12}+k^2\zeta_{-11}\phi_{12}-\phi_{-11yy}\zeta_{12}-\zeta_{-11}\phi_{12yy}$$
$$+\Omega\zeta_{-11}\zeta_{11\eta}-\phi_{03y}=0,\quad y=0, \tag{A25}$$
$$-\left(c_{\mathrm{g}}-U\right)\phi_{01\eta\eta}-\mathrm{i}\left(\omega-kU\right)\phi_{11\eta y}\zeta_{-11}-\mathrm{i}\left(\omega-kU\right)\phi_{11y}\zeta_{-11\eta}+k^2\phi_{11}\phi_{-11\eta}+\phi_{11y}\phi_{-11\eta y}+g\zeta_{02\eta}$$
$$-2\mathrm{i}k\Omega\zeta_{11}\phi_{-11\eta}+\Omega\phi_{03y}-k^2\Omega\zeta_{11}\phi_{-12}-k^2\Omega\phi_{11}\zeta_{-12}+\Omega\phi_{11yy}\zeta_{-12}+\Omega\zeta_{11}\phi_{-12yy}=0,\quad y=0. \tag{A26}$$

The solutions can be obtained as follows:

$$\phi_{03y}=-\left(y+h\right)\phi_{01\eta\eta}, \tag{A27}$$
$$\left[\left(c_{\mathrm{g}}-c\bar{u}\right)\left(c_{\mathrm{g}}-c\bar{u}+\Omega h\right)-gh\right]\phi_{01\eta}=\left[\frac{k\omega\left(2+X-2\bar{u}\right)\left(1+X-\bar{u}\right)}{\left(1-\bar{u}\right)\left(1+N\right)}+k^2\left(1-\sigma^2\right)\left(c_{\mathrm{g}}-c\bar{u}\right)\right]|A|^2, \tag{A28}$$
$$g\zeta_{02}=\left(c_{\mathrm{g}}-c\bar{u}+\Omega h\right)\phi_{01\eta}-k^2\left(1-\sigma^2\right)|A|^2. \tag{A29}$$

For $m=3$ and $n=1$, the governing equations are

$$2ik\phi_{12\eta}+\phi_{11\eta\eta}-k^2\phi_{13}+\phi_{13yy}=0,\quad -h<y<\zeta, \tag{A30}$$
$$\phi_{13y}=0,\quad y=-h, \tag{A31}$$
$$\zeta_{11\tau}-\left(c_{\mathrm{g}}-U\right)\zeta_{12\eta}-\mathrm{i}\left(\omega-kU\right)\zeta_{13}+2k^2\phi_{-11}\zeta_{22}+2k^2\zeta_{-11}\phi_{22}+\mathrm{i}k\zeta_{11}\phi_{01\eta}+k^2\phi_{-11y}\zeta_{11}^2-\phi_{13y}-\phi_{11yy}\zeta_{02}$$
$$-\phi_{-11yy}\zeta_{22}-\zeta_{-11}\phi_{22yy}-\phi_{11yyy}\zeta_{-11}\zeta_{11}-\frac{1}{2}\phi_{-11yyy}\zeta_{11}^2+\mathrm{i}k\Omega\zeta_{11}\zeta_{02}+\mathrm{i}k\Omega\zeta_{-11}\zeta_{22}=0,\quad y=0, \tag{A32}$$
$$-\mathrm{i}\left(\omega+kc_{\mathrm{g}}-2kU\right)\phi_{12\eta}+k\left(\omega-kU\right)\phi_{13}+\mathrm{i}k\phi_{11\tau}+k\left(\omega-kU\right)\phi_{11y}\zeta_{02}-k\left(\omega-kU\right)\phi_{-11y}\zeta_{22}$$
$$+2k\left(\omega-kU\right)\zeta_{-11}\phi_{22y}+\frac{3}{2}k\left(\omega-kU\right)\phi_{11yy}\zeta_{11}\zeta_{-11}-\left(c_{\mathrm{g}}-U\right)\phi_{11\eta\eta}-k^2\phi_{01\eta}\phi_{11}+2\mathrm{i}k^3\phi_{-11}\phi_{22}-\mathrm{i}k^3\phi_{11}\phi_{11y}\zeta_{-11}$$
$$+\mathrm{i}k^3\phi_{11}\phi_{-11y}\zeta_{11}+\mathrm{i}k^3\phi_{-11}\phi_{11y}\zeta_{11}+\mathrm{i}k\phi_{-11y}\phi_{22y}+\mathrm{i}k\phi_{11yy}\phi_{11y}\zeta_{-11}+\mathrm{i}k\phi_{-11yy}\phi_{11y}\zeta_{11}+\mathrm{i}k\phi_{11yy}\phi_{-11y}\zeta_{11}$$
$$-4k^2\Omega\zeta_{-11}\phi_{22}-k^2\Omega\phi_{11}\zeta_{02}-k^2\Omega\phi_{-11}\zeta_{22}+k^2\Omega\phi_{-11y}\zeta_{11}^2-k^2\Omega\phi_{11y}\zeta_{11}\zeta_{-11}+\Omega\phi_{11yy}\zeta_{02}$$
$$+\Omega\phi_{-11yy}\zeta_{22}+\Omega\zeta_{-11}\phi_{22yy}+\frac{1}{2}\Omega\phi_{11yyy}\zeta_{11}\zeta_{-11}\Omega\phi_{13y}+g\left(1+3N\right)\zeta_{12\eta}+\mathrm{i}gk\left(1+N\right)\zeta_{13}$$
$$-\mathrm{i}\frac{3\upsilon k}{\rho}\zeta_{11\eta\eta}-\mathrm{i}\frac{3\upsilon k^5}{2\rho}\zeta_{11}^2\zeta_{-11}=0,\quad y=0. \tag{A33}$$

Solving Eqs. (A30)–(A31) and using solvability conditions

[Eqs. (A32)–(A33)], we can reach the NLSE of gravity-capillary waves with a linear shear flow for the amplitude A of the velocity potential, as given in the text.

References

[1] Zheng G Z, Cong P X and Pei H Y 2006 *J. Geophys. Res.* **111** C11016
[2] Zhang T and Song J B 2018 *Adv. Atmos. Sci.* **35** 469
[3] Zakharov V E 1972 *J. Appl. Math. Tech. Phys.* **9** 190
[4] Benney D J and Roskes G 1969 *Stud. Appl. Math.* **48** 377
[5] Hasimoto H and Ono H 1972 *J. Phys. Soc. Jpn.* **33** 805
[6] Davey A and Stewartson K 1974 *Proc. R. Soc. Lond. A* **338** 101
[7] Djordjevic V D and Redelopp L G 1977 *J. Fluid Mech.* **79** 703
[8] Li J C, Hui W H and Donelan M A 1988 *Nonlinear Water Waves* (Berlin: Springer-Verlag) pp. 213–220
[9] Thomas R, Kharif C and Manna M 2012 *Phys. Fluids* **24** 127102
[10] Hsu H C, Kharif C, Abid M and Chen Y Y 2018 *J. Fluid Mech.* **854** 146
[11] Li S F, Chen J, Cao A Z and Song J B 2019 *Chin. Phys. B* **28** 124701
[12] Abid M, Kharif C, Hsu H C and Chen Y Y 2019 *J. Fluid Mech.* **871** 1028
[13] Zhang J and Melville W K 1986 *Wave Motion.* **8** 439
[14] Tiron R and Choi W 2012 *J. Fluid Mech.* **696** 402
[15] Vanden-Broeck J M and Dias F 1992 *J. Fluid Mech.* **240** 549
[16] Longuet-Higgins M S 1989 *J. Fluid Mech.* **200** 451
[17] Kang Y and Vanden-Broeck J M 2000 *Eur. J. Mech. B Fluids* **19** 253
[18] Gao T, Wang Z and Milewski P A 2019 *J. Fluid Mech.* **876** 55
[19] Akers B and Milewski P A 2009 *Stud. Appl. Math.* **122** 249
[20] Akers B and Milewski P A 2010 *SIAM. J. Appl. Math.* **70** 2390
[21] Wang Z and Milewski P A 2012 *J. Fluid Mech.* **708** 480
[22] Milewski P A and Wang Z 2014 *Proc. R. Soc. A* **470** 20130537
[23] Dorio J D, Cho Y, Duncan J H and Akylas T R 2011 *J. Fluid Mech.* **672** 268
[24] Park B and Cho Y 2016 *J. Fluid Mech.* **808** 168
[25] Masnadi N and Duncan J H 2017 *J. Fluid Mech.* **814** R1
[26] Zhang X 1995 *J. Fluid Mech.* **289** 51
[27] Zhang X 1999 *Eur. J. Mech. B Fluids* **18** 373
[28] Liao B, Dong G, Ma Y and Gao J L 2017 *Phys. Rev. E.* **96** 043111
[29] Zhao L C and Ling L M 2016 *J. Opt. Soc. Am. B* **33** 850
[30] Ling L M, Zhao L C, Yang Z Y and Guo B L 2017 *Phys. Rev. E* **96** 022211
[31] Baronio F, Conforti M, Degasperis A, Lombardo S, Onorato M and Wabnitz S 2014 *Phys. Rev. Lett.* **113** 034101
[32] Baronio F, Chen S H, Grelu P, Wabnitz S and Conforti M 2015 *Phys. Rev. A* **91** 033804
[33] Ablowitz M J and Segur H 1979 *J. Fluid Mech.* **92** 691
[34] Benjamin T B and Hasselmann K 1967 *Proc. R. Soc. Lond. A* **299** 59
[35] Wang D L, Yan X H and Tang Y 2004 *J. Phys. Soc. Jpn.* **73** 123